

NOTES AND CORRESPONDENCE

A Simple Atmospheric Correction Model for ROCSAT-2 RSI Data

Chien-Hui Liu^{1,*}

(Manuscript received 16 May 2003, in final form 16 October 2003)

ABSTRACT

A simple atmospheric correction model (SACM) for ROCSAT-2 RSI data is presented. Gaseous transmission and Rayleigh optical depth are simplified as analytic functions. Rayleigh and aerosol scattering are determined using lookup tables. Results indicate that SACM not only quite accurately reproduces top-of-atmosphere reflectance computed by the 6S model (Vermote et al. 1997), but also does so faster than 6S. The results of the inverse application of SACM also indicate that the error of surface reflectance can be greatly reduced even in hazy sky if the adjacency effect is corrected. Future studies and possible improvements are also highlighted.

(Key words: Atmospheric correction model, ROCSAT-2, Reflectance, Adjacency effect)

1. INTRODUCTION

The ROCSAT-2 satellite will be launched in the end of 2003 to image over Taiwan and the surrounding area daily for various applications, such as agriculture, land use and disaster monitoring (Lee et al. 2002). It is in a sun-synchronous orbit (inclination angle 98.99°) descending over (120°E , 24°N) and 9:45 a.m. over the equator. The Remote Sensing Instrument (RSI) on board will provide images for 2 m ground sampling distance (GSD) in panchromatic band and 8 m GSD in four Landsat-like multispectral bands. Figure 1 shows the sensor response functions from band 1 to band 4 of ROCSAT-2 RSI. Their central wavelengths correspond to 0.484 (blue), 0.561 (green), 0.660 (red) and 0.817 (near-infrared) μm , respectively. The central wavelength λ_c of every spectral band is determined by

¹Department of Information Management/Geographic Information Management and Research Center, Transworld Institute of Technology, Taiwan

*Corresponding author address: Prof. Chien-Hui Liu, Department of Information Management/Geographic Information Management and Research Center, Transworld Institute of Technology, 1221, Jen. S. Rd., Douliu, Yunlin 64045, Taiwan; E-mail: chliu@tit.edu.tw

$$\lambda_c = \int \lambda S(\lambda) E(\lambda) d\lambda / \int S(\lambda) E(\lambda) d\lambda,$$

where $S(\lambda)$ and $E(\lambda)$ are sensor response function and exoatmospheric solar irradiance, respectively (Vermote et al. 1997). The RSI will take four-strip images covering the whole of Taiwan during one pass by viewing in $\pm 45^\circ$ for along-track and cross-track. Since satellite sensors receive signals not only by reflection from a target but also by atmospheric scattering and absorption, the atmospheric correction of ROCSAT-2 RSI data is necessary to retrieve the land parameters, such as vegetation indices (VIs), leaf area index (LAI) and land use/land cover change. The process of converting raw data to surface reflectance requires the atmospheric correction model. Hence, it's very important to develop the atmospheric correction model for ROCSAT-2 RSI data.

The atmospheric correction of numerous remotely sensed data requires a fast, accurate, and even operational atmospheric correction model. Many researchers have successfully developed such models using the simplified method and/or lookup table approach. Using the simplified functions for gaseous transmission, atmospheric reflectance, spherical albedo and scattering transmission, top-of-atmosphere (TOA) reflectance can be accurately simulated (at approximately 0.001) (Rahman and Dedieu 1994) a few hundred or even several thousand times faster than 5S as developed by Tanre et al. (1990). In fact, some other researchers also developed fast and accurate atmospheric correction algorithms using various radiative transfer codes, such as the 5S code by Zagolski and Gastellu-Etchegorry (1995) and the MODTRAN code (Berk et al. 1989) by Richter (1997). The accuracy and limits on the developed models are confined by not only the radiative transfer code itself but also the way researchers implement the code. For example, Liang et al. (1997) determined lookup tables only at discrete wavelengths, whereas Richter (1997) integrated the atmospheric functions with the sensor spectral response function. Some models do not correct the adjacency effect on high resolution images such as Landsat TM images (Liang et al. 1997). Although ATCOR3 (Richter

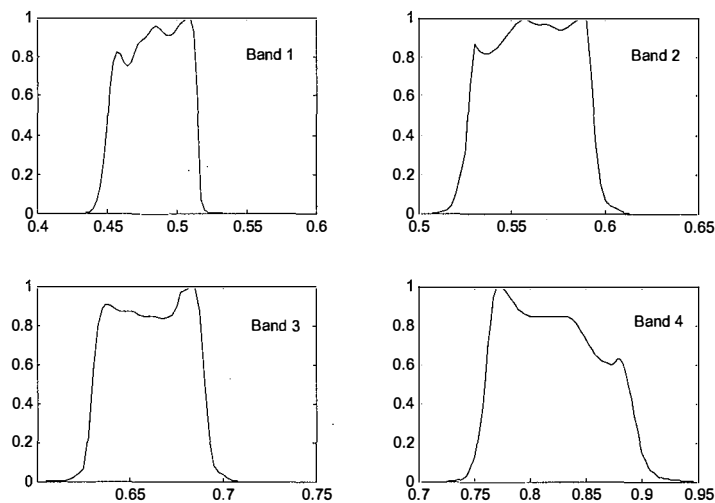


Fig. 1. Sensor response functions from band 1 to band 4 of ROCSAT-2 RSI.

1997) successfully demonstrate an ability to correct both atmospheric and topographic effects on Landsat TM and SPOT HRV images over a wide range of atmospheric conditions, the azimuthal dependence of atmospheric functions is simplified (relative azimuthal angles of 30 and 150 degrees) to keep down the size of the lookup table for SPOT images. The altitude-dependence of atmospheric functions is also usually neglected (Rahman and Dedieu 1994). Consequently, retrieval of surface reflectance may not be accurate, especially for high resolution ROCSAT-2 RSI data over the mountainous area of Taiwan.

In this paper, a simple atmospheric correction method (SACM) for ROCSAT-2 RSI data is developed. The 6S radiative transfer code (Vermote et al. 1997) is used, because it is accurate and has been successfully used in the development of an atmospheric correction model for EOS MODIS (Vermote et al. 2002) data. Since SACM utilizes simplified functions for gaseous transmission and Rayleigh optical depth and lookup tables for atmospheric scattering, it can rapidly (several hundred times faster than 6S) and accurately (~ 0.001) reproduce TOA reflectance. When SACM is used in the inverse mode, it can also convert the TOA reflectance to surface reflectance with correction of adjacency effect.

2. SIMPLE ATMOSPHERIC CORRECTION METHOD (SACM)

SACM is based on the 6S radiative transfer model, whose outputs are considered to determine simplified functions for gaseous transmission and Rayleigh optical depth, and lookup tables for Rayleigh and aerosol scattering. It considers various altitudes (but not on sloped terrain) and can correct the adjacency effect. The approach somewhat follows the methodology of Vermote et al. (2002). All of the transmission functions and scattering lookup tables of the various gases and aerosol are computed by 6S and spectrally integrated with the sensor response functions for the four bands of ROCSAT-2 RSI. For simplicity, only the continental aerosol model is considered here.

3. RESULTS AND DISCUSSIONS

Several experiments have been conducted to validate SACM. These compare gaseous transmission, scattering terms and TOA reflectance obtained by SACM and 6S. The experiments also show the advantage of SACM over 6S in terms of execution speed, as well as the correction of the adjacency effect.

The performance of SACM is evaluated in terms of maximum relative error (MRE) and root mean square error with respect to 6S. The MRE is defined as $100|X_i - X_{6S}|/X_{6S}$ and $\text{rmse} = \sqrt{(X_i - X_{6S})^2 / (N - 1)}$, with X_i derived by SACM and X_{6S} according to 6S. Such validation is analogous to that employed by Rahman and Dedieu (1994).

3.1 Gaseous Transmissions and Rayleigh Optical Depth

Table 1 presents the regressed coefficients of the simplified functions of ozone, water

vapor, oxygen transmissions and Rayleigh optical depth for various bands of ROCSAT-2 RSI. The corresponding MRE and rmse values are also calculated. 6S is used at various ranges to evaluate the fitness of the simplified functions. Tropical atmosphere is used. Both solar zenith angle θ_s and viewing zenith angle θ_v are from 0° to 60° , and therefore the air mass varies from 2 to 4. Ozone content in sea level $U_{O_3}(0)$ is varied from 0.1 to 0.6 cm-atm to evaluate the performance of ozone transmission $T_{g_{O_3}}$. The MRE values are 0.0000, 0.0001, 0.0001, 0.0000 and 0.0004 % from band 1 to band 5 and the corresponding rmse values are all the same as those of MRE. These results indicate that the ozone transmission calculated by SACM agrees very well with that of 6S for all bands.

The simulated water vapor transmission $T_{g_{H_2O}}$ values obtained with water vapor content in sea level $U_{H_2O}(0)$ from 1.0 to 10.0 g cm⁻² are also compared with those of 6S. The MRE values are all 0.0000 for all bands except 0.0001 for band 4, and the corresponding rmse values are all 0.0000 for all bands. The MRE and rmse values of $T_{g_{H_2O}}$ with $U_{H_2O}(0)/2$ are of the same order with those of $T_{g_{H_2O}}$ values obtained with $U_{H_2O}(0)$, although the MRE and rmse values exceed those of transmission with full water vapor content for band 2, band 4 and band 5. These results demonstrate a very good agreement between the water vapor transmission determined by SACM and that by 6S.

The absorption of gases other than ozone and water vapor, including carbon dioxide, oxygen and methane, are relatively unimportant in the spectral bands of ROCSAT-2 RSI. The oxygen transmission as a function of the product of airmass and the ratio of pressure to sea level pressure is determined for band 3, band 4 and band 5. Airmass varies from 2 to 4. Oxygen content is equal to one since the concentration is effectively constant (Rahman and Dedieu 1994). Altitude ranges from 0 to 3.2 km. The MRE and rmse values are 0.0000 for band 3, band 4 and band 5, which indicates the good agreement between SACM and 6S for oxygen transmission computation.

Rayleigh optical depth τ_R as a function of altitude for the tropical atmospheric model is also determined. Altitude varies from 0 to 7 km. Although the MRE values are all 0.0117%, the rmse values are only 0.0008, 0.0004, 0.0002, 0.0001 and 0.0003 from band 1 to band 5, which depicts τ_R computed by SACM agrees very well with that by 6S.

The above discussion shows that the gaseous transmission and Rayleigh optical depth computed by SACM agree very closely with those by 6S.

3.2 Lookup Tables for Rayleigh and Aerosol Scattering

To assess the performance of the lookup tables for atmospheric spherical albedo S , diffuse transmittance of molecules $t_d^R(\mu)$, diffuse transmittance of aerosol $t_d^A(\mu)$, environment function $F(r)$, atmospheric reflectance of Rayleigh ρ_R and atmospheric reflectance of aerosol ρ_A , these scattering components are computed at two altitudes (0 and 4 km), three solar zenith angles θ_s (0° to 60° , every 30°), 4 viewing zenith angles θ_v (0° to 45° , every 15°), 4 relative azimuthal angles ϕ (0° to 180° , every 60°), and 4 aerosol optical depths (550 nm) (0.05 to 0.8, every 0.25). The aerosol model is continental type. It should be noticed that these scattering components are computed in conditions different from those in the lookup tables. Therefore, the errors of Rayleigh and aerosol scattering are due to interpolation using these lookup tables

Table 1. The regressed coefficients of the simplified functions of ozone, water vapor, oxygen transmissions and Rayleigh optical depth for various bands of ROCSAT-2 RSI. Air mass ranges from 2 to 4. $U_{O_3}(0)$ ranges from 0.1 to 0.6 cm-atm. $U_{H_2O}(0)$ ranges from 1.0 to 10.0 g cm⁻². For other gases, altitude ranges from 0 to 3.2 km. Tropical atmospheric is used.

		Band 1	Band 2	Band 3	Band 4	Band 5	
O ₃	a	0.0190	0.0948	0.0565	0.0007	0.0427	
	a	-26.6444	-5.9611	-6.0626	-3.8764	-4.5883	
H ₂ O*	b	0.5488	1.0104	1.0195	0.7054	0.7794	
	c	-0.0579	-0.0589	-0.0508	-0.0332	-0.0405	
	a	-26.6444	-6.6655	-6.7634	-4.4027	-5.1581	
H ₂ O [#]	b	0.5488	1.0742	1.0676	0.7676	0.8432	
	c	-0.0579	-0.0557	-0.0468	-0.0361	-0.0419	
	a	-	-	0.0106	0.0219	0.0097	
O ₂	b	-	-	0.4699	0.3471	0.3628	
	τ_R	$\tau_R(0)$	0.1700	0.0925	0.0474	0.0203	0.06923
		H_{τ_R}	7.8357	7.8357	7.8357	7.8357	7.8357

*: for U_{H₂O}; #: for U_{H₂O}/2.

as compared with the values calculated by 6S under the same afore-mentioned conditions.

The MRE values and the rmse values of atmospheric scattering terms are computed. The rmse values of $t_d^R(\mu)$ and ρ_R are less than 0.0002 and 0.0003 from band 1 to band 5, although their MRE values are all greater than 1.0 %. The rmse values of $t_d^A(\mu)$ are 0.0040, 0.0033, 0.0026, 0.0015 and 0.0015 from band 1 to band 5, which exceed an order of magnitude higher than those of $t_d^R(\mu)$. The MRE values of $t_d^A(\mu)$ are also larger than those of $t_d^R(\mu)$. One would have noticed that the rmse values of $t_d^A(\mu)$ are the largest compared with those of other scattering terms. However, the overall errors of TOA reflectance ρ_{TOA} are around 0.001 for all bands, as one can see in the following discussions. Even though the MRE values of ρ_A can reach 30.43, 10.86, 7.908, 7.454 and 9.564 from band 1 to band 5, their corresponding rmse values are only 0.0008, 0.0007, 0.0006, 0.0004 and 0.0006, respectively. The MRE values of

S are all less than 1.0 % for all bands except band 4, and the rmse values are all around 0.0007. The MRE values of $F(r)$ are all less than 1.0 % for all bands, and the rmse values are all very low (0.0000).

The rmse values of all scattering components are relatively low, and thus lead to the satisfactorily accurate simulation of TOA reflectance by SACM, as described in the following section.

3.3 The Accuracy Assessment of the Simulation of TOA Reflectances by SACM

Figure 2 compares TOA reflectances ρ_{TOA} simulated by SACM and 6S for band 1, band 3, band 4 and band 5. Wide ranges of parameters are set as follows to determine the accuracy of SACM: altitude z varies from 0 to 4.0 km; θ_s and θ_v vary from 0° to 60° and from 0° to 45° respectively; ϕ varies from 0° to 180° ; $U_{O_3}(0)$ and $U_{H_2O}(0)$ vary from 0.1 to 0.7 cm-atm and from 0.5 to 7.0 g cm⁻², respectively; AOD varies from 0.05 to 0.8; the aerosol model is of the continental type, and three target reflectance ρ_s and background reflectance ρ_b values (0.05, 0.25 and 0.45) are used. The MRE values of ρ_{TOA} are 2.413, 2.416, 2.471, 2.376 and 3.072 % from band 1 to band 5, and the corresponding rmse values are less than 0.001 (0.0008, 0.0007, 0.0006 and 0.0006 from band 1 to band 5, respectively) except for band 5 (0.0016). From the

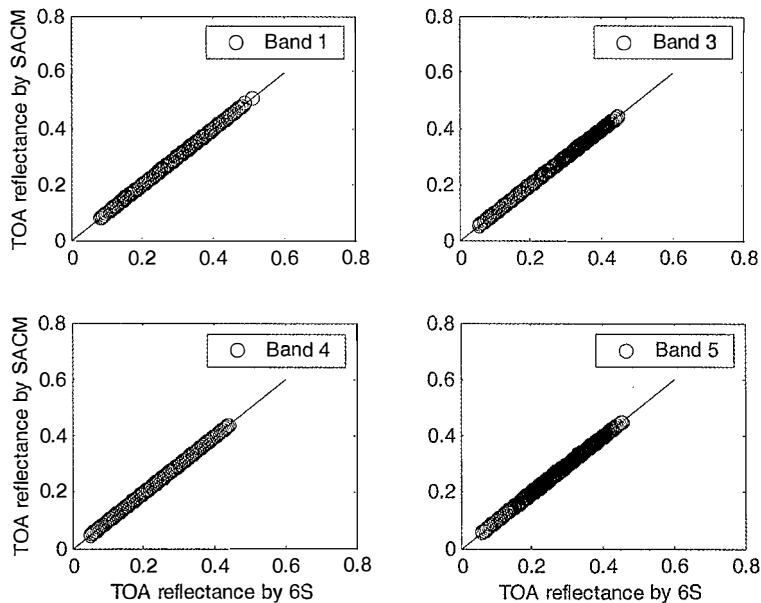


Fig. 2. Comparison between the TOA reflectances as determined by 6S and SACM for various bands of ROCSAT-2 RSI. θ_s ranges from 0° to 60° , θ_v from 0° to 45° , ϕ from 0° to 180° and AOD from 0.05 to 0.8. $U_{O_3}(0)$ and $U_{H_2O}(0)$ vary from 0.1 to 0.7 cm-atm and from 0.5 to 7.0 g cm⁻². Aerosol optical depth varies from 0.05 to 0.8. The altitude is from 0 to 4.0 km. Surface and background reflectances are 0.05, 0.25, and 0.45.

above discussions, therefore, SACM can mimic 6S with sufficient accuracy.

Table 2 compares the CPU time required for 1024 runs of TOA reflectance calculation for various bands using 6S and SACM on a personal computer (Pentium 4 with 1.7 GHz CPU). The computational time required for 6S varies significantly with spectral bands and is almost constant for SACM. For band 1, SACM is 614 times faster than 6S and for band 4 it is 425 times more rapid. For panchromatic band (band 5), SACM is 1191 times more rapid than 6S. One can see that as the bandwidth increases the computational time for 6S increases because of the necessity of the spectral integration. Hence, SACM is also appropriate for correcting the atmospheric effects of ROCSAT-2 RSI data.

3.4 Determination of Surface Reflectance with Correction for the Adjacency Effect

Figure 3 presents the example of simulation of TOA reflectance and atmospherically corrected surface reflectance with/without correction of adjacency effect by SACM for spectral bands of ROCSAT-2 RSI. Vegetation surface (target) has assumed to be surrounded by soil surface (background). Both vegetation and soil reflective spectra refer to spectral reflectances for different dry green biomass levels for alfalfa canopy (Fig. 10 of Deering (1989)). θ_s , θ_v and ϕ are 60° , 45° and 180° , respectively. $U_{O_3}(0)$ and $U_{H_2O}(0)$ are 0.3 cm-atm and 4.0 g cm^{-2} , respectively. Visibility is 5 km. The altitude is in sea level. As one can see in Fig. 3, TOA reflectances are much higher than surface reflectances in blue, green and red bands of ROCSAT-2 RSI. It's because of the stronger atmospheric scattering effect for the short wavelengths. TOA reflectance in near-infrared band is lower than the surface reflectance mainly due to the aerosol and water vapor absorption. Therefore, this emphasizes again the necessity of the atmospheric correction of remotely sensed signal. When the atmospheric effect has been corrected without considering the adjacency effect, i.e. uniform surface assumption, the retrieved vegetation spectral reflectances are much closer to the surface

Table 2. Comparison of CPU time (seconds) required for 1024 iterations of TOA reflectance calculation for different bands of ROCSAT-2 RSI using 6S and SACM on a personal computer (Pentium 4 with 1.7 GHz CPU).

Band	6S	SACM
1	1842	3
2	1818	3
3	1751	3
4	1275	3
5	3574	3

reflectances, although there still exist some deviations. Such deviations, which are due to the atmospheric forward scattering from the background (soil), can be reduced if the adjacency effect is corrected.

This experiment reveals the necessity of correcting for the adjacency effect on high-resolution ROCSAT-2 RSI data.

4. CONCLUSIONS

The main contributions of this paper are the development of the simple atmospheric correction model (SACM) suited to ROCSAT-2 RSI data. Compared with 6S, SACM is reasonably accurate and much faster, and thus can be applied to satellite receiving stations for the atmospheric correction of ROCSAT-2 RSI data in near real time.

It should be emphasized that an accurate atmospheric correction model may not correct the atmospheric effects well on numerous remotely sensed data without knowledge of the

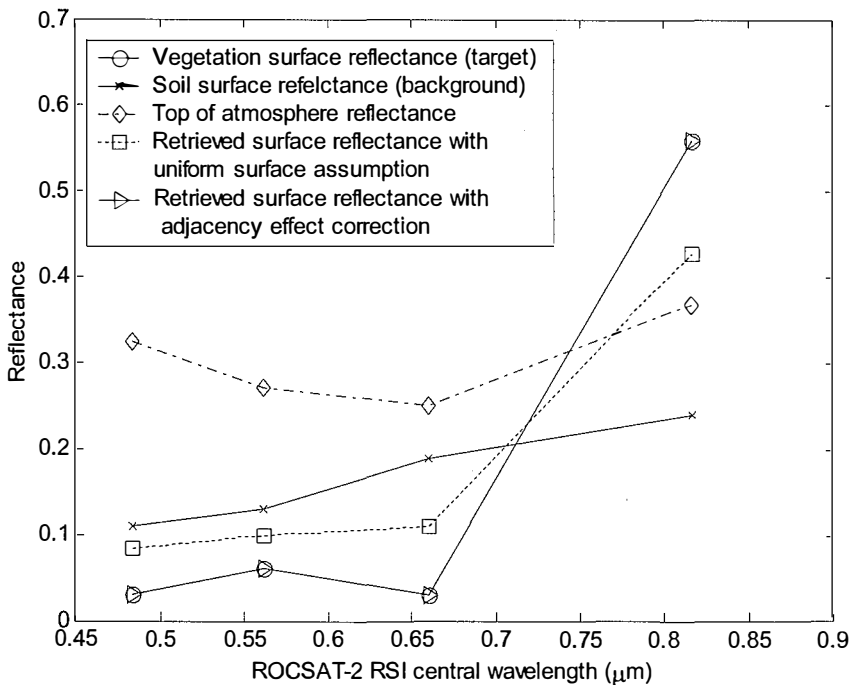


Fig. 3. Example of simulation of top of atmosphere reflectance and atmospherically corrected surface reflectance with/without correction of adjacency effect by SACM for spectral bands of ROCSAT-2 RSI. Vegetation surface (target) has assumed to be surrounded by soil surface (background). θ_s , θ_v and ϕ are 60° , 45° and 180° , respectively. $U_{O_3}(0)$ and $U_{H_2O}(0)$ are 0.3 cm-atm and 4.0 g cm^{-2} , respectively. Visibility is 5 km . The altitude is in sea level.

atmospheric parameters (Rahman and Dedieu 1994), particularly the aerosol concentration, due to its spatial and temporal variation. To be operational, the only method to obtain the aerosol concentration of ROCSAT RSI data is to retrieve the AOD from the image itself. Although the dark target (DT) approach has been operationally applied to Landsat TM (Liang et al. 1997) and EOS MODIS data (Vermote et al. 2002), the contrast reduction (CR) based methods, such as “structure method” (Lin et al. 2002) and “dispersion method” (Liu et al. 2002), can be alternative ways to successfully estimate the AOD from the complex terrains for SPOT HRV and NOAA AVHRR data. The major assumptions of the DT approach are the existence and referenced reflectances in visible bands of DT, and those of the CR method are unchanged ground reflectances within multi-temporal data and the difference between the data satisfactorily attributed to the difference of AOD. In considering the four bands of ROCSAT-2 RSI, both methods are suitable. However, further investigation is suggested. Nevertheless, SACM can be used inversely to retrieve AOD by using both approaches, since it is fairly accurate and fast.

Currently, SACM adopts only the continental aerosol model, which is not appropriate for urban pollution, fog or even Asian dust storms, which are very active in spring. Although altitude dependence is considered, SACM does not consider the topographic effects of a sloped surface also. Future work will improve SACM accordingly.

Acknowledgements The author is grateful to Mr. Sz-Yuan Lee at National Space Program Office for his help on the spectral response functions of the ROCSAT-2 RSI. The anonymous reviewers’ comments led to significant improvements in the manuscript. This work was supported by the Taiwan National Science Council under grant NSC91-2212-E-265-001.

REFERENCES

- Berk, A., L. S. Bernstein, and D. C. Robertson, 1989: MODTRAN: a moderate resolution model for LOWTRAN 7, GL-TR-89-0122, Geophysics Laboratory, Bedford, MA, U. S. A.
- Deering, D. W., 1989: Field measurements of bidirectional reflectance. In: Theory and Applications of Optical Remote Sensing, G. Asrar (Eds.), John Wiley & Sons, 37-38.
- Lee, Y. Y., A. M. Wu, and F. Wu, 2002: An algorithm for geometric correction of high resolution image based on physical modeling. In *the 23rd Asian Conference on Remote Sensing*, 23-29 November 2002, Nepal.
- Liang, S., H. Fallah-Adl, S. Kalluri, J. Jaja, Y. J. Kaufman, and J. R. G. Townshend, 1997: An operational atmospheric correction algorithm for Landsat Thematic Mapper imagery over the land. *J. Geophys. Res.*, **102(D14)**, 17173-17186.
- Lin T. H., A. J. Chen, G. R. Liu, and T. H. Kuo, 2002: Monitoring the atmospheric aerosol optical depth with SPOT data in complex terrain. *Int. J. Remote Sens.*, **23**, 647-659.
- Liu G. R., T. H. Lin, and T. H. Kuo, 2002: Estimation of aerosol optical depth by applying the optimal distance number to NOAA AVHRR data. *Remote Sens. Environ.*, **81**, 247-252.
- Rahman, H., and G. Dedieu, 1994: SMAC: a simplified method for the atmospheric correction of satellite measurements in the solar spectrum. *Int. J. Remote Sens.*, **15**, 123-143.

- Richter, R., 1997: Correction of atmospheric and topographic effects for high spatial resolution satellite imagery. *Int. J. Remote Sens.*, **18**, 1099-1111.
- Tanre, D., C. Deroo, P. Duhaut, M. Herman, J.-J. Morcrette., J. Perbos, and P. Y. Deschamps, 1990: Description of a computer code to simulate the satellite signal in the solar spectrum: the 5S code. *Int. J. Remote Sens.*, **11**, 659-668.
- Vermote, E. F., Nazmi Z. El Saleous, and C. O. Justice, 2002: Atmospheric correction of MODIS data in the visible to middle infrared first results. *Remote Sens. Environ.*, **83**, 97-111.
- Vermote, E. F., D. Tanre, J. L. Deuze, M. Herman, and J.-J. Morcrette, 1997: Second simulation of the satellite signal in the solar spectrum, 6S: an overview. *IEEE Trans. Geosc. Remote Sens.*, **35(3)**, 675-686.
- Zagolski, F., and J. P. Gastellu-Etchegorry, 1995: Atmospheric corrections of AVIRIS with a procedure based on the inversion of the 5S model. *Int. J. Remote Sens.*, **16**, 3115-3146.